Restricted epithelial proliferation by lacritin via PKCα-dependent NFAT and mTOR pathways

Jiahu Wang,[1] Ningning Wang,[1] Jinling Xie,[1] Staci C. Walton,[1] Robert L. McKown,[3] Ronald W. Raab,[3] Peisong Ma,[1] Shannon L. Beck,[1] George L. Coffman,[3] Isa M. Hussaini,[2] and Gordon W. Laurie[1]

[1]Department of Cell Biology and [2]Department of Pathology, University of Virginia, Charlottesville, VA 22904
[3]Department of Integrated Science and Technology, James Madison University, Harrisonburg, VA 22807

Renewal of nongermative epithelia is poorly understood. The novel mitogen "lacritin" is apically secreted by several nongermative epithelia. We tested 17 different cell types and discovered that lacritin is preferentially mitogenic or prosecretory for those types that normally contact lacritin during its glandular outward flow. Mitogenesis is dependent on lacritin's C-terminal domain, which can form an α-helix with a hydrophobic face, as per VEGF's and PTHLP's respective dimerization or receptor-binding domain. Lacritin targets downstream NFATC1 and mTOR. The use of inhibitors or siRNA suggests that lacritin mitogenic signaling involves $G\alpha_i$ or $G\alpha_o$–PKCα-PLC–Ca^{2+}–calcineurin–NFATC1 and $G\alpha_i$ or $G\alpha_o$–PKCα-PLC–phospholipase D (PLD)–mTOR in a bell-shaped, dose-dependent manner requiring the Ca^{2+} sensor STIM1, but not TRPC1. This pathway suggests the placement of transiently dephosphorylated and perinuclear Golgi–translocated PKCα upstream of both Ca^{2+} mobilization and PLD activation in a complex with PLCγ2. Outward flow of lacritin from secretory cells through ducts may generate a proliferative/secretory field as a different unit of cellular renewal in nongermative epithelia where luminal structures predominate.

Introduction

The stem cell niche is a key characteristic of germative epithelia. Renewal of nongermative epithelia is by definition much more challenging to address. Yet, nongermative epithelia comprise most adult organs of the body, including exocrine and endocrine glands, kidney, and liver (Rizvi and Wong, 2005). Recent cell lineage studies in the adult endocrine pancreas suggested that differentiated β-cells are renewed by self-duplication rather than via stem cells (Dor et al., 2004). General applicability to other nongermative epithelia has not been explored. However, this observation is in keeping with early [^{3}H]TdR incorporation studies of exocrine and endocrine pancreas, liver, trachea, kidney, and the salivary, thyroid, and adrenal glands (Messier and Leblond, 1960). A dynamically regulated state of differentiation is suggested by successful nuclear transfer from differentiated donor cells, and by the fusibility of differentiated muscle and brain cells with bone marrow stem cells (Sacco et al., 2005). If nongermative epithelia are broadly proliferative, one implication is that mitogenic stimuli are correspondingly widely dispersed—much like the luminal distribution of differentiative hedgehog along the intestinal villus axis.

The human mitogen lacritin is preferentially associated with nongermative epithelia. Lacritin is apically secreted by acinar cells in the adult lacrimal gland and by a subpopulation of ductal cells in salivary glands (Sanghi et al., 2001), and it has been detected by nonhistological methods in thyroid (Sanghi et al., 2001) and mammary glands (Weigelt et al., 2003) and some ocular surface cells, but not elsewhere. Acinar lumina and long ducts transport lacritin past apical membranes of the nongermative epithelia comprising both glands. Later, lacritin is deposited onto the rapidly renewing epithelia on the surface of the eye and mouth, where it can be detected by ELISA. Thus, instead of localized release to nurture crypt stem cells, as per Wnts, lacritin is apically secreted for broad distribution. Lacritin may therefore stimulate epithelia in its downstream path. Supporting this hypothesis are in vitro studies showing recombinant lacritin to be capable of promoting lacrimal acinar cell secretion, human salivary ductal cell proliferation, and Ca^{2+} mobilization by human corneal epithelial (HCE) cells (Sanghi et al., 2001). Thus, release of lacritin may hypothetically define

J. Wang, N. Wang, and J. Xie contributed equally to this paper.

Correspondence to Gordon W. Laurie: glaurie@virginia.edu

Abbreviations used in this paper: CsA, cyclosporin A; HCE, human corneal epithelial; HSG, human salivary ductal; PLD, phospholipase D; PM, plasma membrane; PNG, perinuclear Golgi region; PTX, pertussis toxin; SF, serum-free; SOC, store-operated Ca^{2+}.

The online version of this article contains supplemental material.

The Journal of Cell Biology, Vol. 174, No. 5, August 28, 2006 689–700
http://www.jcb.org/cgi/doi/10.1083/jcb.200605140

a combined secretory and proliferative field that spreads through the nongermative epithelia of lacrimal and salivary glands. Because other nongermative epithelia have luminal structures, secretory/proliferative fields might be a general principle.

We sought to characterize lacritin's domain, cell target specificity, optimal dose, and signaling pathways. We determine that lacritin targets only a small subset of epithelia, and not fibroblasts or glia. It does so via a C-terminal domain, which, in parallel studies (Ma et al., 2006), appears to require heparanase (HPSE) to unblock a binding site in the core protein of coreceptor syndecan-1 (SDC1). Lacritin signaling to PKCα activates both Ca^{2+}–NFAT and phospholipase D (PLD)–mTOR pathways via the Ca^{2+} sensor STIM1, suggesting a novel mitogenic approach for renewal.

Results

Lacritin is a cell-selective mitogen

Lacritin flows over nongermative glandular epithelia of acini and ducts to later become deposited on the surface of the eye or mouth (Fig. 1 A). The human salivary ductal (HSG) cell response to recombinant lacritin is bell-shaped with an optimal dose of 1 or 10 nM (Fig. S1, available at http://www.jcb.org/cgi/content/full/jcb.200605140/DC1), promoting a level of proliferation often matching the FBS-positive control (Fig. 1 B). This biphasic response and dosage is equivalent to that seen for sonic hedgehog, VEGF, FGF, and PDGF in other cell systems (Chang et al., 2004). Few other cell types are targeted by lacritin. Lacritin is mitogenic for HCE and human embryonic kidney cells (Fig. 1 B), which both display a similar bell-shaped response (unpublished data). Lacritin does not appear to be mitogenic for human epidermal (A431), cervical (HeLa), foreskin fibroblast (HS68), fibrosarcoma (HT1080), erythroleukemia (K-562), noninvasive breast carcinoma (MCF7), melanoma (SK-MEL and WM-164), Leydig (TM4), Sertoli (TM3), and mouse fibroblast (NIH3T3) cells (Fig. 1 B), or for human glioma (U-1242-MG and U-251-MG) cells, even at higher doses (unpublished data). Lacritin targeting is rapid. Lacritin signaling is apparent within the first minute by differential and transient tyrosine phosphorylation of at least nine different unidentified phosphoproteins (Fig. 1 C) in an equivalent dose-responsive manner (unpublished data) that exceeds the moderately high level of endogenous phosphorylation that is characteristic of these cells. [^{3}H]TdR uptake is also rapid, and it is detectable within 2 h of lacritin addition (unpublished data). Interestingly, p42 and p44 MAPK do not appear to be activated (Fig. 1 D), thereby minimizing the possibility that lacritin-dependent mitogenesis involves transactivation of the EGF pathway, or of another common Ras–MAPK cytokine or growth factor pathway.

Lacritin's C terminus drives mitogenesis

Such cell target specificity is unusual. Porter et al. (2003) suggested that the putative breast cancer oncogene dermcidin is a homologue of lacritin. Comparing both by near optimal alignment revealed three weakly homologous regions in the C-terminal half (Smoot et al., 2005), two of which reside in predicted α-helices (Fig. 2). Several C- and one N-terminal truncation mutants were therefore generated (Fig. 2 A). Mutants lacking 5 and 10 aa from the C terminus, or 24 aa from the N terminus, were fully active. Removal of 5 or 10 more C-terminal amino acids (C-15 or C-20), respectively diminished or completely abrogated activity (Fig. 2 B, shown at 10 nM). This pattern is mirrored by loss of binding to the core protein of lacritin coreceptor SDC1 (Ma et al., 2006). Thus, the 10 additional C-terminal amino acids deleted from C-10 (aa 100–109 of mature lacritin; Fig. 2 C) are important for both activities. To determine whether

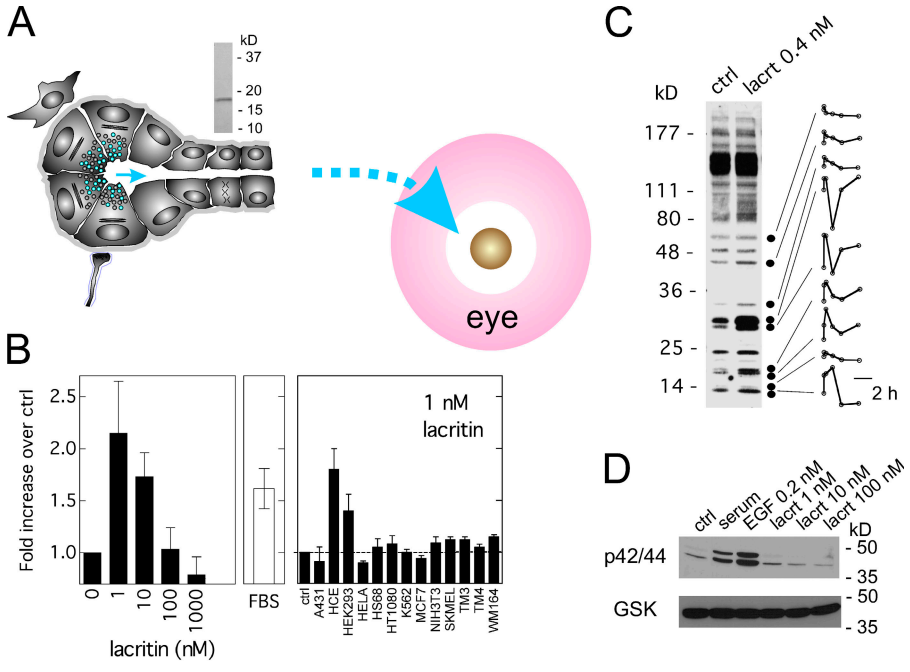

Figure 1. **Cell target specificity of mitogenic lacritin.** (A) Lacritin released from lacrimal acinar cell secretory granules flows via ducts to the surface of the eye. In the salivary gland, lacritin is generated by ductal cells and flows into saliva. Observations are based on ELISA detection of lacritin in human tears or saliva, and immunolocalization of lacritin in human lacrimal and salivary glands (Sanghi et al., 2001). (top) Mature recombinant lacritin purified from *Escherichia coli* and pLAC construct. (B) Lacritin targeting of HSG cells promotes a bell-shaped mitogenic response with maximum proliferative activity at 1 or 10 nM lacritin, similar to that of the 10% FBS–positive control. Lacritin also targets downstream HCE and human embryonic kidney 293 cells. Cell types that were not responsive include the following: A431, HeLa, HS68, HT1080, K562, MCF7, NIH3T3, SKMEL, TM3, TM4, or WM164 cells. In other studies, lacritin promotes secretion and Ca^{2+} mobilization by rat (Sanghi et al., 2001) and rabbit (unpublished data) lacrimal acinar cells. (C) Tyrosine phosphorylation before and 1 min after lacritin addition. Accompanying densitometric scans follow tyrosine phosphorylation over 4 h. (D) p42/p44 are not activated by lacritin. Loading control is total glycogen synthase kinase β. All experiments performed in HSG cells in this and subsequent figures.

this region is capable of α-helical formation, we synthesized the active region KQFIENGSEFAQKLLKKFS with several flanking amino acids and subjected it to circular dichroism. In PBS it formed a random coil, and in 10 mM dodecylphosphocholine it formed an α-helix (Fig. 2 D). Although plasma membrane (PM) insertion is not in keeping with lacritin's low nanomolar activity and cell specificity, hydrophobic surfaces on the same or different proteins can create an environment appropriate for α-helical formation (Murre et al., 1989). By "helical wheel," 5 of 10 residues in the active region are hydrophobic, and all group along one face (Fig. 2 E) as an amphipathic α-helix. Amphipathic α-helices are common in ligand–receptor or ligand–ligand interactions. The hydrophobic face of PTHLH's C-terminal amphipathic α-helix, for example, mediates binding of PTHR1 (Barden et al., 1997). The same mechanism directs VEGF dimerization as a prerequisite for FLT1 and KDR receptor binding (Siemeister et al., 1998).

Distinctive lacritin mitogenic signaling through PKCα

How does lacritin signal toward mitogenesis? Lacritin-targeted HCE cells rapidly mobilize intracellular Ca^{2+} (Sanghi et al., 2001), and in HSG cells, tyrosine phosphorylation of at least nine unidentified proteins follows within a minute of lacritin addition (Fig. 1 C). p42 and p44 activation were excluded (Fig. 1 D), suggesting that lacritin mitogenic signaling was likely distinct from the Ras–MAPK pathway common to many growth factors and cytokines. Although lacritin binds SDC1 (Ma et al., 2006), its demonstrated signaling properties are limited. Loading HSG cells with the Ca^{2+} indicator Fluo-4 (Fig. 3) revealed that the mitogenic dose of lacritin (10 nM), but not of nonmitogenic C-25 deletion mutant, usually promotes Ca^{2+} mobilization within 30 s of addition (Fig. 3, A–C, and E). Several common inhibitors were tested (Fig. 3 C). Preincubation with 100 ng/ml pertussis toxin (PTX) completely inhibited mobilization, suggesting an upstream requirement for active G proteins $G\alpha_i$ or $G\alpha_o$. Cells treated with positive control muscarinic agonist carbachol were unaffected (Fig. 3 C). Carbachol's $G\alpha_q$-mediated pathway is well known to be insensitive to PTX. The aminosteroid U73122 was tested next. U73122 inhibits G protein–mediated activation of PLC that, in turn, catalyzes the formation of IP_3 and DAG. 1 μM U73122 inhibited Ca^{2+} mobilization by both lacritin and carbachol (Fig. 3 C), suggesting that PLC-generated IP_3 directs Ca^{2+} release from intracellular stores. To test this hypothesis, cells were incubated in 2-[^{3}H]myo-inositol for 24 h and then stimulated. IP_3 generation was detected within 15 s of adding lacritin or carbachol. None was formed with C-25 (Fig. S2, available at http://www.jcb.org/cgi/contents/full/jcb.200605140/DC1). DAG activates downstream PKC. Yet, when cells were preincubated with 1 μM of the PKC inhibitor Go 6976, lacritin-stimulated Ca^{2+} mobilization was completely inhibited (Fig. 3 C), suggesting an unusual upstream requirement for active PKC. In contrast, mobilization was unaffected in positive control carbachol-stimulated cells (Fig. 3 C), even at 10 μM Go 6976 (unpublished data). Therefore, lacritin signaling displays distinctive features.

Davies et al. (2000) demonstrated that specificities of protein kinase inhibitors are less narrow than initially thought. Although Go 6976 is the most selective of PKC inhibitors, in vitro assays reveal the capacity to inhibit elements of the MAPK (MKK1 and MAPKAP-K1b), ERK/p38 (MSK1), Rho (ROCK2), and Akt (S6K1) pathways, as well as GSK3B downstream of $G\alpha_q$. HSG cells are known to express PKCα, δ, ε, γ, ι, and λ (Jung et al., 2000), of which only the α isoform should be inhibited by Go 6976 at 1 μM. PKCα mRNA was thus targeted for degradation by RNAi (Fig. 4). HSG cells were transfected with a pool of four siRNAs for PKCα. PKCα became depleted, and transfected cells failed to proliferate in response to lacritin. Serum-triggered mitogenesis was slightly reduced ("D7–D10") in comparison to mock and negative controls. Cells were then individually transfected with each of the four siRNAs. Both PKCα D7 and D10 transfectants were lacritin unresponsive, but completely serum responsive in proliferation assays (Fig. 4). Importantly, further testing of D7 revealed no lacritin-dependent Ca^{2+} mobilization (Fig. 3 C; bottom). We hypothesize that ligation of coreceptor SDC1 (Ma et al., 2006) is coupled to binding of a G protein–coupled receptor, thereby successively activating $G\alpha_i$ or $G\alpha_o$, PKCα, and PLC.

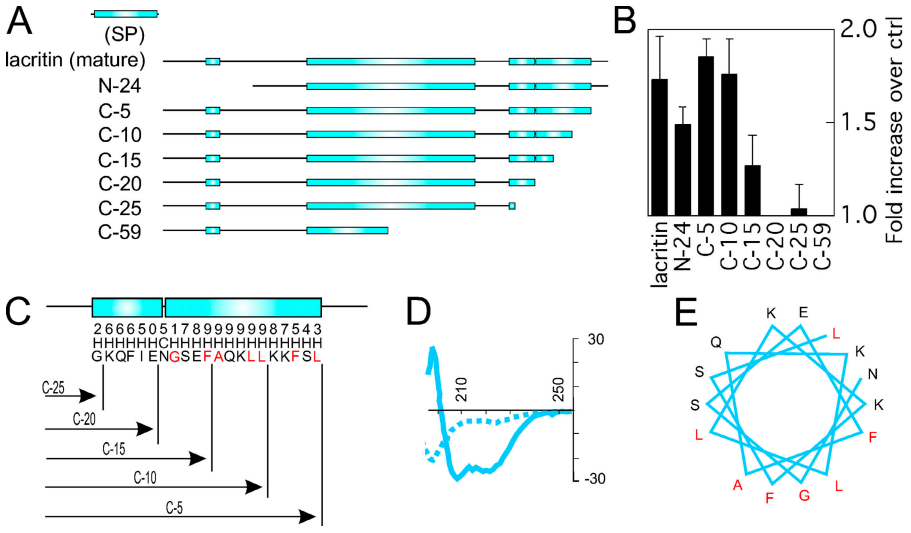

Figure 2. **Lacritin's C-terminal α-helix is necessary for mitogenesis.** (A) Mature lacritin versus N- and C-terminal deletion constructs. Boxed are PSIPRED-predicted α-helices. (B) Deletion constructs N-24, C-5, C-10, and C-15 are active; C-20, C-25, and C-59 are inactive. Concentration of lacritin and lacritin deletion constructs is 10 nM in this and subsequent figures. (C) Activity breakpoint suggests that the proximal 2/3 of the more distal of two predicted C-terminal α-helices is essential for mitogenesis. A predicted N-linked glycosylation site (NGS) binds the N terminus of the distal helix. PSIPRED confidence numbers for an α-helix (H) or random coil (C) are indicated. (D) KQFIENGSEFAQKLLKKFS forms a random coil in PBS (dashed line) and an α-helix in 10 mM dodecylphosphocholine (solid line), as examined by circular dichroism. (E) The C-terminal α-helix (NGSEFAQKLLKKFS) likely presents the hydrophobic-binding face "AFGL," as predicted by the helical wheel.

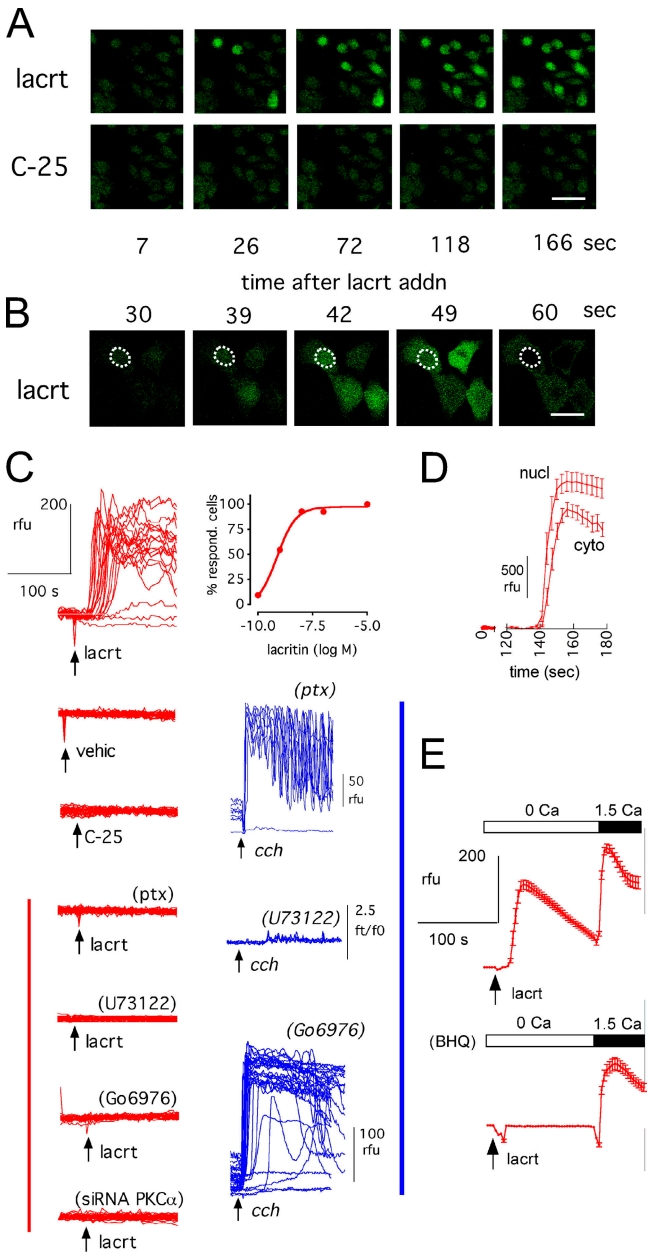

Figure 3. **Lacritin's mitogenic C terminus promotes Ca^{2+} mobilization in a PTX-inhibitable manner that requires PLC and PKCα.** (A) Mobilization of intracellular Ca^{2+} 20–30 s after lacritin (lacrt), but not C-25, addition (cells in Ca^{2+}-containing medium for this and subsequent figures, unless indicated otherwise). (B) Apparent initial nuclear mobilization (circled) or a combination of cytoplasmic and nuclear mobilization because this is the thickest part of the cell. (C) Ca^{2+} fluorescence tracings after addition (arrow) of lacritin, C-25, vehicle (vehic), or positive control carbachol (cch) in the absence or presence of inhibitors. Ca^{2+} mobilization in response to lacritin is observed in most cells per field at 1 or 10 nM and is suppressed by pretreatment with PTX, U73122, Go 6976, or by siRNA depletion of PKCα. Carbachol-dependent mobilization is unaffected by PTX or Go 6976. (D) Fluorescence quantitation of apparent nuclear (see note in (B) above) versus cytoplasmic signal (11–17 cells). (E) Ca^{2+} mobilization with or without Ca^{2+} and 10 μM BHQ pretreatment. Cells pretreated with BHQ in Ca^{2+}-free medium just before the addition of 10 nM lacritin in the same medium (18–27 cells). Bars: (A) 50 μm; (B) 25 μm.

Ca^{2+} can be mobilized from sources both inside and outside cells. Several simple experiments were performed to gain insight. Stimulating cells in Ca^{2+}-free medium mobilized Ca^{2+},

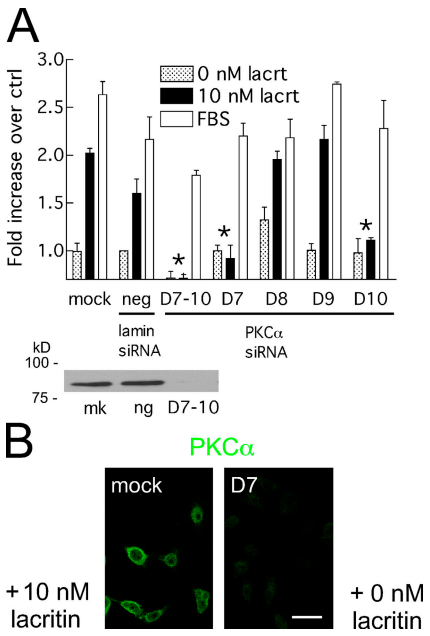

Figure 4. **PKCα is necessary for lacritin-dependent mitogenesis.** (A) siRNA depletion of PKCα eliminates lacritin's mitogenic response, as observed with pooled siRNAs D7–10, and D7 and D10 applied individually. Little or no effect on FBS-stimulated mitogenesis, or on negative control lamin A/C siRNA, is observed. PKCα blot illustrates protein depletion with D7–10, but not in mock-transfected (mk) or lamin A/C siRNA-transfected cells (ng). Data are presented as the mean ± the SEM. Asterisks represent inhibitory siRNAs. (B) PKCα knockdown via D7 is visualized by anti-PKC immunofluorescence. Bar, 50 μm.

suggesting internal release. Restoration of extracellular Ca^{2+} promoted further mobilization (Fig. 3 E), suggesting influx. BHQ was tested next. BHQ reversibly inhibits the sarcoplasmic reticulum Ca^{2+}/Mg^{2+} ATPase, thereby preventing refilling and allowing depletion of intracellular ER Ca^{2+} stores. 10 μM BHQ pretreatment inhibited Ca^{2+} mobilization by lacritin (Fig. 3 E), suggesting that ER Ca^{2+} stores are targeted by lacritin signaling, in keeping with lacritin-dependent IP_3 generation (Fig. S2). Store-operated Ca^{2+} (SOC) influx is the movement of Ca^{2+} across the PM in response to depleted Ca^{2+} stores (Ambudkar, 2006; Putney, 2005). High concentration 2-APB is an inhibitor of SOC influx. When 100 μM 2-APB was added to lacritin- or thapsigargin-treated cells at maximal mobilization, suppression was immediate (unpublished data). TRPC channels (including TRPC1 in HSG cells; Liu et al., 2000) have been proposed to be essential for SOC. In two recent comprehensive and independent siRNA screens for SOC mediators, the major hits were to STIM1 and STIM2 (Roos et al., 2005; Liou et al., 2005). To determine whether STIM1 or TRPC1 may play a role in lacritin-dependent Ca^{2+} influx, HSG cells were depleted of each by siRNA. Lacritin stimulation of cells in nominally Ca^{2+}-free media, followed by Ca^{2+} addition, revealed that influx was suppressed in STIM1-depleted cells (Fig. S3, available at http://www.jcb.org/cgi/contents/full/jcb.200605140/DC1). Influx in cells lacking TRPC1 appeared unaffected. Collectively, these results suggest that PKCα plays a central role in lacritin mitogenic signaling, and that STIM1, but not TRPC1, may be necessary for Ca^{2+} influx, possibly via a SOC mechanism.

This pattern was later confirmed in NFAT translocation and mitogenesis experiments.

Lacritin stimulates translocation of PKCα to the perinuclear Golgi region (PNG)

PKCα regulation of cell proliferation is initiated by translocation of cytoplasmic PKCα to membranes. Interaction of membrane-associated PKCα with other membrane-associated effectors drives downstream signaling to mitogenesis. To appreciate how lacritin mitogenic signaling is transduced in the context of Ca^{2+} mobilization, we asked whether lacritin promotes PKCα translocation and, if so, to which membrane compartment. PKCα was imaged in cells 15 min after treatment (Fig. 5 A). 10 nM nonmitogenic C-25 had no effect, leaving PKCα diffusely distributed throughout the cytoplasm. In contrast, 10 nM lacritin or N-24 shifted PKCα primarily to the PNG, as confirmed by colocalization with the Golgi marker mannosidase II (Fig. 5 B). Cells treated with positive control PMA concentrated PKCα solely in the PM (unpublished data). The phosphorylation state of PKCα influences its translocation site. Hyperphosphorylated PKCα becomes associated with the PM, whereas hypophosphorylated or dephosphorylated PKCα is known to translocate to the PNG (Hu and Exton, 2004). To determine if the latter is true and, if so, over what time course, cells were treated with lacritin, N-24, and C-25. Cell lysates were then blotted for phospho-PKCα (Fig. 6). 10 nM lacritin promotes PKCα dephosphorylation within 1 min of addition. This form is sustained for at least 15 min, but by 30 min has returned to baseline phosphorylation. Dephosphorylation triggered by increasing molar levels of lacritin or N-24 mirrored the proliferation response, with optimal dephosphorylation at 1 or 10 nM. Nonmitogenic C-25 had no effect, whereas positive control PMA promoted some phosphorylation. It was suggested that lacritin-stimulated signaling toward Ca^{2+} mobilization follows a $G\alpha_i$ or $G\alpha_o$–PKCα–PLC pathway. If so, PTX and Go 6976, but not U73122 should inhibit PKCα translocation. We retested each and observed that lacritin-dependent PKCα translocation and dephosphorylation were inhibited by 100 ng/ml PTX and 1 μM Go 6976, but also by 1 μM U73122 (Fig. 5 A). The weakly active analogue U73343 is often used as a negative control for U73122. Cells preincubated with 1 μM U73343 displayed full translocation (Fig. 5 A). This implies that an interdependent complex of PKCα and PLC may be intermediate between $G\alpha_i$ or $G\alpha_o$ activation and PKCα translocation, most logically in the PM. Yet as early as 1 min, PKCα was dephosphorylated, and therefore likely already translocated to the PNG. An alternative possibility is that a PLC isomer is stationed in the PNG and when active serves to capture translocating PKCα. PLCγ2 is concentrated in the PNG in mast cells before and after antigen stimulation (Barker et al., 1998). Is PLCγ2 or another PLC isomer located in the PNG of HSG cells and, if so, does it complex with PKCα? Cells were treated for 15 min with 10 nM lacritin, and then immunostained for PKCα and PLCγ2 (Fig. 7). PLCγ2 displays a discrete perinuclear Golgi localization, which partially overlaps with PKCα (Fig. 7 A), suggesting that the two are in sufficient proximity to form a signaling complex. The existence of a PLCγ2–PKCα complex was, including some

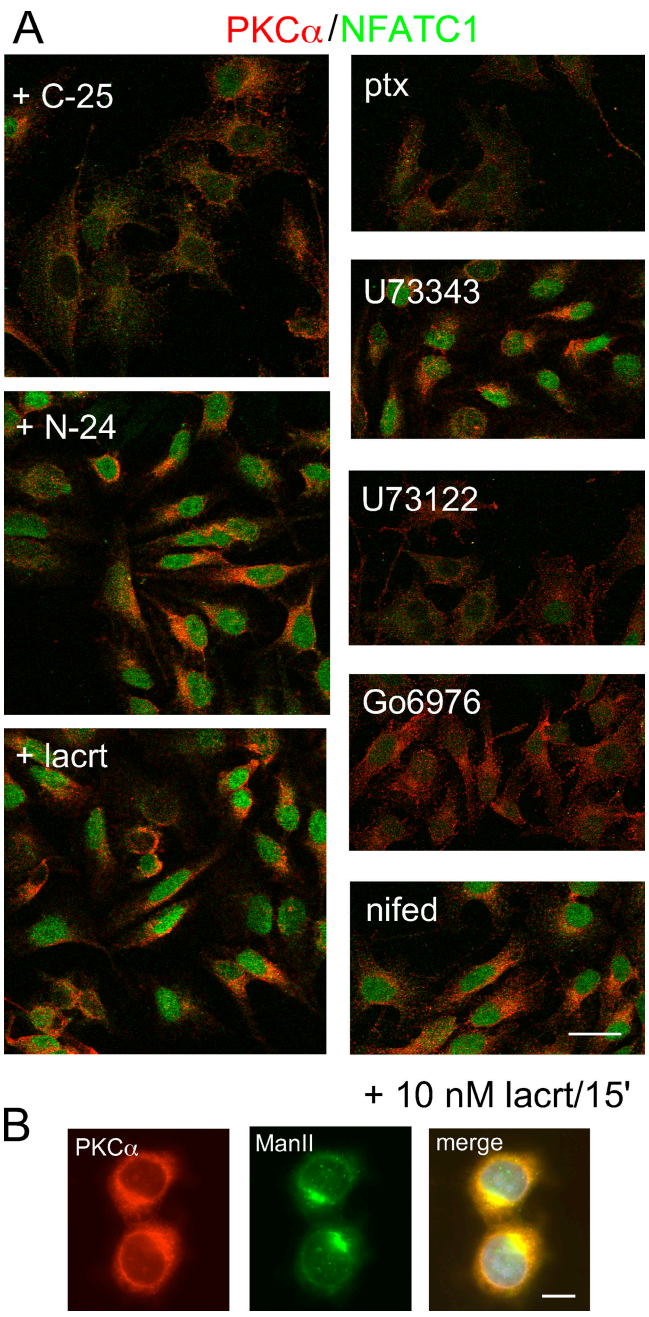

Figure 5. **Lacritin stimulates translocation of PKCα to the PNG and NFATC1 to the nucleus, both in a $G\alpha_i$- or $G\alpha_o$- and PLC-dependent manner.** (A) Lacritin and N-24, but not C-25, promotes translocation of PKCα to the PNG and NFATC1 to the nucleus. Lacritin-dependent translocation of PKCα and NFATC1 are inhibited by PTX, U73122, and Go 6976; but not by inactive U73122 analogue U73343, nor nifedipine (nifed). Translocation at 15 min with 10 nM lacritin is shown. Bar, 25 μm. (B) Translocated PKCα partially colocalizes with the Golgi marker mannosidase II (ManII; same time and dose as in A). Bar, 10 μm.

activated PLCγ2, confirmed by anti-PLCγ2 immunoprecipitation (Fig. 7, B and C).

Downstream activation of PLD

We propose that translocation of hypophosphorylated PKCα to the PNG is anchored by an interdependent complex with active PLCγ2. Local generation of IP_3 then may drive Ca^{2+}

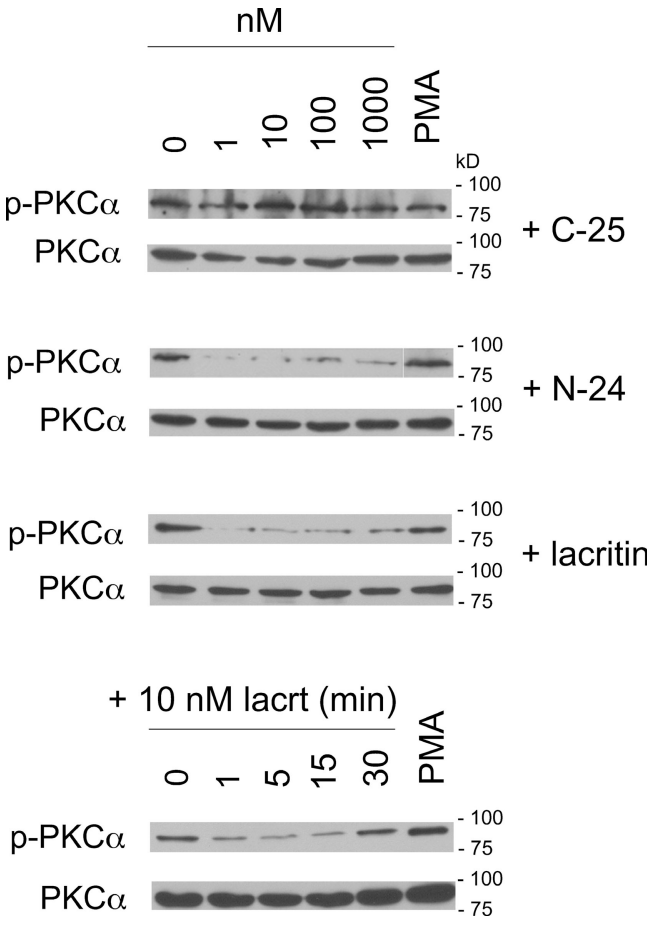

Figure 6. **Lacritin-dependent PKCα dephosphorylation is temporally linked with perinuclear Golgi translocation.** Western blots illustrating dose- and time-dependent dephosphorylation of PKCα in response to lacritin or N-24, but not C-25. Total PKCα protein serves as loading control.

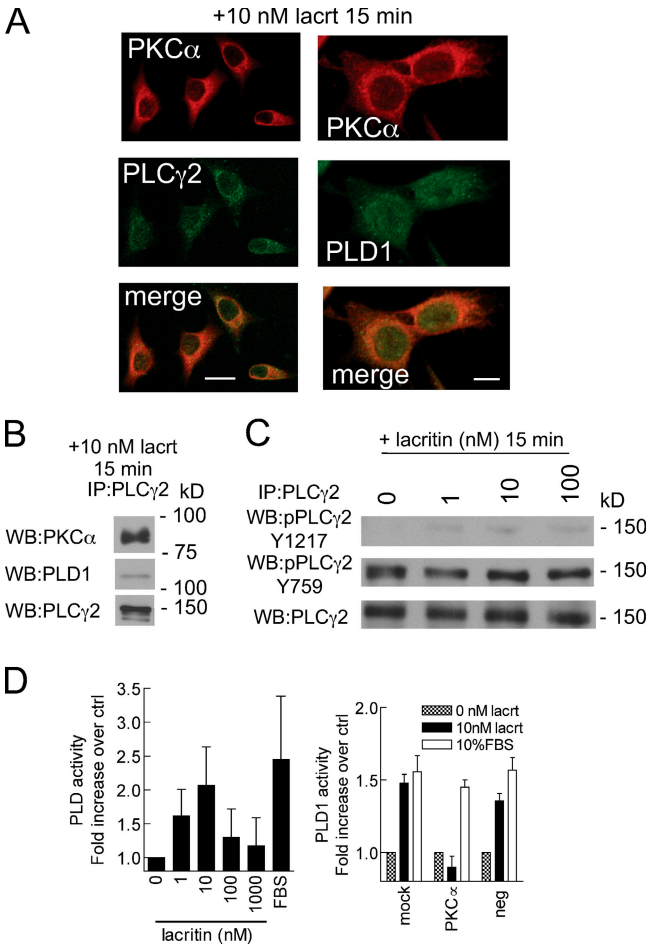

Figure 7. **Translocated PKCα becomes associated with PLCγ2 and activates PLD1.** (A) Perinuclear colocalization of PKCα with PLCγ2; and PKC with PLD1 15 min after lacritin addition. Bars, 25 μm (left) and 10 μm (right). (B) Anti-PLCγ2 immunoprecipitate of homogenate from cells treated for 15 min with lacritin contains PKCα and PLD1. (C) Lacritin dose–response analysis of PLCγ2 phosphorylation in anti-PLCγ2 immunoprecipitates of homogenate from 15-min–treated cells. (D) Lacritin addition promotes activation of PLD in a biphasic dose-dependent manner. Activation is abrogated by knockdown of PKCα using siRNA D7, which has little or no effect on FBS-stimulated PLD activation. Data are presented as the mean ± the SEM.

mobilization, followed by extracellular Ca^{2+} entry via a STIM1-regulated mechanism. Could other effectors be activated from this site? Recently, Hu and Exton (2004) linked perinuclear translocation of hypophosphorylated PKCα to activation of PLD1 via a protein–protein interaction. PLD1 is most concentrated in the PNG and plays a key role in cell proliferation and secretion (for review see Foster and Xu, 2003), which are both functions of lacritin. Therefore, we hypothesized that lacritin-stimulated translocation of hypophosphorylated PKCα activates perinuclear Golgi PLD to, in turn, generate phosphatidic acid by hydrolysis of phosphatidylcholine. Endogenous PLD activity was measured. After lacritin addition, PLD displays a bell-shaped activation curve that was optimal at 10 nM lacritin (Fig. 7 D), thus, recapitulating the same dose dependency observed for mitogenesis, PKCα translocation, and PKCα dephosphorylation. To ask whether PKCα was upstream of PLD in lacritin signaling, cells were transfected with D7 siRNA. Depletion of PKCα completely abrogated PLD activation in response to lacritin, whereas PLD activation by serum was unaffected (Fig. 7 D). By confocal microscopy, PLD1 displays a broader perinuclear, and partially nuclear, distribution that partially colocalizes with PKCα in lacritin-stimulated cells (Fig. 7 A). Both are detected in anti-PLCγ2 immunoprecipitates (Fig. 7 A). Therefore, it appears that transiently hypophosphorylated perinuclear Golgi PKCα complexes with PLCγ2 to perform at least two roles. It triggers IP_3 generation and Ca^{2+} mobilization, and it also activates PLD1.

Common upstream signals diverge

Downstream lacritin signaling toward cell cycle progression may follow at least two different pathways. First, the prominence of Ca^{2+} mobilization raises the possibility that cytoplasmic Ca^{2+} may stimulate the phosphatase calcineurin to activate cytoplasmic NFAT. Dephosphorylated NFAT translocates into the nucleus, where it binds DNA in an obligatory cooperative interaction with other transcription factors including Fos, Jun, GATA, and C/EBP. Second, because lacritin signaling activates PLD1 (Fig. 7 D) and active PLD1 generates phosphatidic acid, it is possible that lacritin signals to the mitogenic phosphatidic acid–mTOR–p70 S6 kinase 1 pathway (Fang et al., 2003).

Hypothetically, both pathways could be additively required for lacritin mitogenesis, as per parallel ERK and mTOR mitogenic signaling in response to FGF-9 (Wing et al., 2005). Alternatively, one may modulate the other, as per PI(3)K/Akt inhibition of calcineurin in muscle IGF-1 signaling (Rommel et al., 2001). The first question was whether calcineurin is activated. Dose response assays revealed that lacritin activated calcineurin in a biphasic manner (Fig. 8 A) within 1 min of addition and was substantially reduced at 30 min (unpublished data). 10 nM nonmitogenic C-25 had no effect, whereas N-24 was activating (Fig. 8 A). Activation was dependent on PKCα and STIM1, but not TRPC1, and was inhibited by cyclosporin A (CsA; Fig. 8 D). Because NFAT in lacrimal, salivary gland, or corneal epithelia has not previously been studied, we chose to examine NFATC1, which is the only NFAT isomer selectively up-regulated in the proliferative compartment of skin epithelium (Tumbar et al., 2004). We localized NFATC1 in cells 15 min after treatment (Fig. 5 A). 10 nM nonmitogenic C-25 had no effect; NFATC1 was diffusely distributed throughout the cytoplasm. In contrast, 10 nM lacritin or N-24 shifted NFATC1 to the nucleus. For verification and to follow the dose response and time course, cells were treated with lacritin, N-24, and C-25, and then purified nuclei blotted for NFATC1 (Fig. 8, B and C). 10 nM lacritin promoted NFAT translocation within 1 min of addition. Translocation was sustained for 30 min. As per PKCα, PLD, and mitogenic responses, 1 or 10 nM lacritin was optimal. In contrast, the Ca^{2+} dose response is sigmoidal (unpublished data). This suggests that a step associated with calcineurin is responsible for the sigmoidal-to-biphasic transition. To ask whether NFATC1 translocation was downstream of $G\alpha_i$ or $G\alpha_o$, PKCα and PLC cells were treated with each of the inhibitors. Translocation was inhibited by PTX, U73122, and Go 6976, but not by the negative control U73343 (Fig. 5 A). Cells transfected with siRNA for PKCα or STIM1 (but not for TRPC1) were also incapable of lacritin-dependent NFATC1 translocation, as were cells in EGTA (Fig. 9 A). This could be quantitated at the cellular level (Fig. S4, available at http://www.jcb.org/cgi/contents/full/jcb.200605140/DC1). As noted, Ca^{2+}-activated calcineurin promotes NFATC1 translocation. CsA inhibits calcineurin (Fig. 8 D). Addition of 1 μM CsA to cells completely blocked lacritin-dependent NFATC1 translocation (Fig. 9 A). To ask whether this pathway is mitogenic, 1 μM CsA was included in the proliferation assay. Other cells were depleted of NFATC1 or STIM1 by siRNA. All three approaches blocked lacritin-stimulated mitogenesis (Fig. 9, C and D). PTX, U73122, and Go 6976, but not U73343, nifedipine (unpublished data), or depletion of TRPC1 (Fig. 9 C), also blocked mitogenesis. Thus, mitogenesis via lacritin-induced NFATC1 translocation appears to be downstream of $G\alpha_i$ or $G\alpha_o$–PKCα-PLC–Ca^{2+}–calcineurin. Moreover, upstream STIM1 appears to be essential as a regulator of Ca^{2+} influx necessary for NFATC1 translocation.

Downstream effectors of activated NFAT include cyclooxygenase-2 (COX2), IL6, and OSCAR, but which effectors would be targeted in HSG cells was unknown. By RT-PCR, only COX2 is affected (Fig. 9 B). Lacritin-induced COX2 expression is inhibited by CsA and reduced in NFATC1-depleted cells. COX2 expression is associated with enhanced epithelial proliferation and decreased apoptosis (Slice et al., 2005).

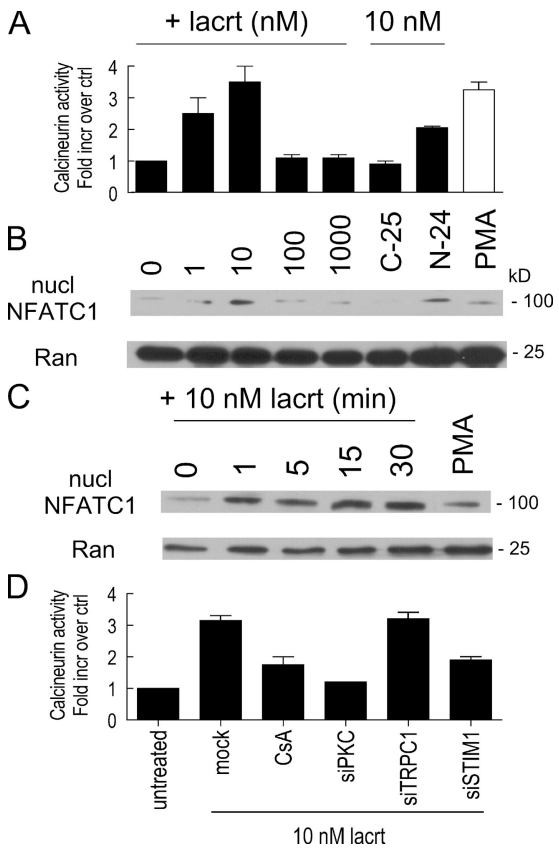

Figure 8. **Time- and dose-dependent activation of calcineurin and appearance of NFATC1 in purified nuclei.** (A) 10 nM lacritin promotes peak calcineurin activity, whereas 10 nM C-25 has no effect. N-24 is also active. (B) Nuclear NFATC1 is detected after treating cells with lacritin or N-24, but not with C-25. Dose response is identical to that for calcineurin. Nuclear protein Ran serves as loading control. (C) Time course for lacritin-dependent NFATC1 translocation. (D) Lacritin-dependent calcineurin activation is inhibited by CsA, and is dependent on PKCα and STIM1, but not TRPC1. Data are presented as the mean ± the SEM.

Recently, Fang et al. (2003) demonstrated that phosphatidic acid generated by PLD1 activates the rapamycin-sensitive mTOR–pS6K1 pathway. mTOR–pS6K1 regulates mitogenicity and cell growth by promoting protein translation necessary for G1 cell cycle transition (Lane et al., 1993). Preincubation of cells with 100 nM of the mTOR inhibitor rapamycin (Fig. 9 D) or depletion of mTOR (Fig. 9 C) by siRNA was inhibitory. Both also suppressed COX2 expression (Fig. 9 B). Recently phospho-activated RSK was found to bind and stabilize an activated NFATC4–DNA complex, thereby contributing to transcriptional activation (Yang et al., 2005). Phosphorylation of RSK is rapamycin-insensitive and downstream of p42/p44. In Fig. 1 D, we showed that p42/p44 is not activated by lacritin. In keeping with this result, no evidence of RSK activation could be detected in lacritin-treated cells (unpublished data). Collectively, these data suggest that mitogenic $G\alpha_i$ or $G\alpha_o$–PKCα-PLC–Ca^{2+}–calcineurin–NFATC1 and $G\alpha_i$ or $G\alpha_o$–PKCα-PLC–Ca^{2+}–calcineurin–PLD1–mTOR pathways are triggered by lacritin via STIM1 activation (Fig. 10).

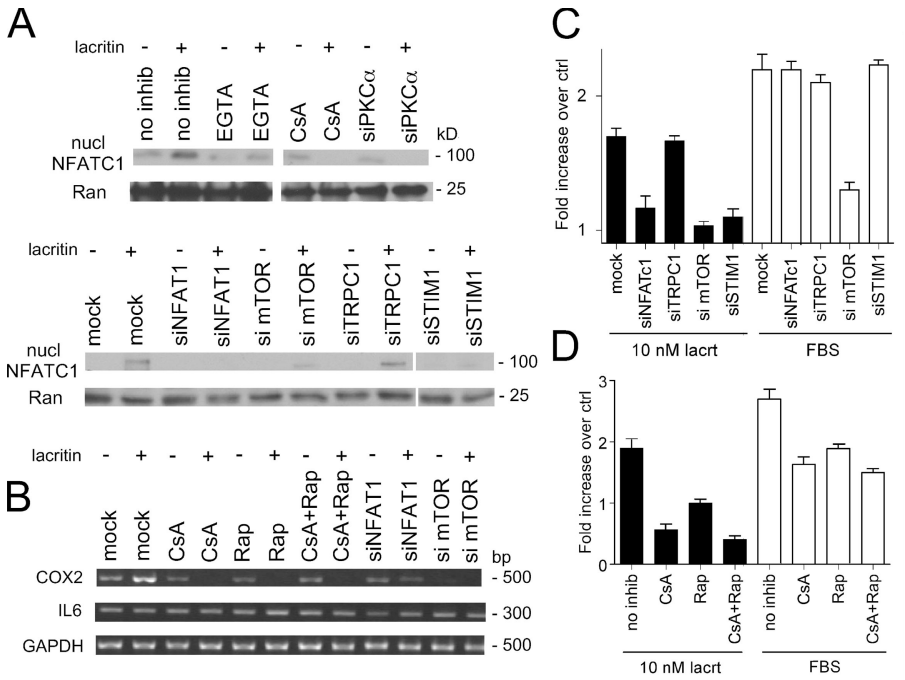

Figure 9. **Ca^{2+} sensor STIM1, but not the Ca^{2+} channel subunit TRPC1, is required for lacritin-dependent NFATC1 translocation and mitogenesis.** (A) Western blots of purified nuclei revealing that lacritin-dependent NFATC1 translocation is inhibited by extracellular EGTA and CsA and requires PKCα and STIM1, but not TRPC1. siRNA depletion of mTOR may slightly decrease NFATC1. (B) Lacritin promotes COX2 mRNA expression downstream of both NFAT and mTOR, as suggested by respective CsA and rapamycin inhibition. Similarly, COX2 expression is decreased or absent in cells depleted of NFATC1 and mTOR. (C) Cells depleted of NFATC1, mTOR, or STIM1, but not TRPC1, display little or no lacritin mitogenesis. (D) CsA and rapamycin both inhibit lacritin-dependent mitogenesis.

Discussion

We document that lacritin is mitogenic for a small subset of epithelial cell lines derived mainly from the nongermative epithelia that normally contact lacritin during its outward glandular flow. This activity is dependent on a C-terminal domain that indirectly activates NFAT and mTOR mitogenic pathways through shared $G\alpha_i$ or $G\alpha_o$, PKCα, PLC, and STIM1-regulated Ca^{2+} signaling (Fig. 10). The possibility that lacritin transactivates another growth factor pathway involving Rho-MAPK appears to be ruled out by lack of MAPK1/MAPK2 and pRSK activation.

Like the Wnt–Ca^{2+} pathway, lacritin signaling is PTX-sensitive and involves NFAT. NFATC1 regulates prostate cancer cell expression of prostate-specific membrane antigen (Lee et al., 2003), smooth muscle proliferation in response to PDGF, and lymphocytic cell cycle progression (Caetano et al., 2002). Linkage of mTOR signaling to cell proliferation has been documented in stem cells of the cerebral cortical proliferative zone (Sinor and Lillien, 2004), CD133(+) bone marrow–derived endothelial precursors (Butzal et al., 2004), and, to a considerable extent, in embryonic stem cells of preimplantation embryos (Gangloff et al., 2004). Thus, each plays key roles in cell proliferation. Upstream PKCα signaling differs. Wnt5a promotes translocation of PKCα to the PM (Sheldahl et al., 1999), whereas lacritin signaling (Fig. 10) appears to stimulate the formation of a transient perinuclear Golgi complex of PKCα, PLD1, and PLCγ2. This activates PLD1 of the mTOR pathway. Some PLCγ2 activation and considerable IP_3 generation were detected. Ca^{2+} mobilization may then be a direct spatiotemporal consequence of PKCα perinuclear Golgi translocation via local generation of IP_3 – thereby placing PKCα upstream of Ca^{2+}. The exact mechanism is unclear. Although supported by PKCα knockdown, Go 6976 suppression can, for example, seem contradictory at first glance. Normally, Go 6976 opposes PKCα phosphorylation as a competitive inhibitor of ATP binding to PKCα's catalytic domain, whereas in lacritin-treated cells the opposite appears to be true. Mirroring our observation, the PKCα inhibitors RO and Bis-1 prevent dephosphorylation of PKCα and translocation to the PNG after PMA treatment of

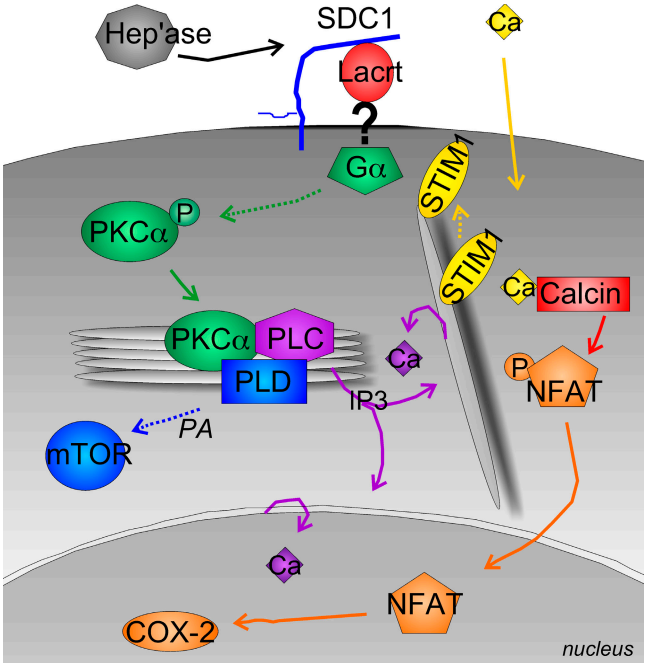

Figure 10. **Proposed model of lacritin mitogenic signaling pathway lacritin signaling suggested by data outlined in the text.** Involvement of HPSE ("Hep'ase") to unblock a lacritin-binding site on SDC1 is from Ma et al. (2006). "?" indicates putative GPCR or ion channel. Dashed lines and items in italics are presumed. PKCα's role upstream of calcineurin (Calcin) is not shown for simplicity.

COS-7 cells (a system in which PKCα translocates to both PM and Golgi). Hu and Exton (2004) accordingly proposed that RO and Bis-1 may be acting as inhibitors of dephosphorylation or inducers of phosphorylation via another protein kinase or phosphatase, as is also likely the case for Go 6976. Interestingly, Go 6976 is also capable of suppressing the activity (Davies et al., 2000) of the mTOR effector and inhibitor S6K1 (Holz and Blenis, 2005), but this is likely inconsequential to lacritin signaling. PKCα is also upstream of calcineurin, and it is possible that biphasic PKCα-dependent regulation of the calcineurin inhibitor DSCR1 may drive calcineurin's biphasic response to lacritin. This would effectively transform the Ca^{2+} sigmoidal response into the observed biphasic mitogenic response.

Lacritin also promotes COX2 expression as a downstream consequence of NFATC1 activation. Both NFAT and mTOR inhibitors appear to suppress expression (Fig. 9 B). This raises the possibility that NFAT and mTOR mitogenic pathways might overlap before COX2 transcription in HSG cells. COX2 is also widely linked to epithelial proliferation and survival (Slice et al., 2005), and, when dysregulated, to epithelial tumors. Mice transgenic for COX2 display sebaceous gland hyperplasia when expression is driven by the keratin 5 promoter (Neufang et al., 2001) and enhanced mammary alveolar differentiation when controlled by the MMTV promoter (Liu et al., 2001). Both conditions are associated with enhanced secretory product (lipid or β-casein, respectively), independent of an effect on cell number. Because lacritin is both mitogenic and prosecretory, it is possible that COX2 might mediate both functions. This possibility is in keeping with new lacritin studies suggesting that the prosecretory and mitogenic dose–response curves might overlap in HCE cells (unpublished data). On the other hand, 10 nM lacritin did not promote amylase expression (unpublished data) by HSG cells that, for mitogenic studies, were routinely plated on plastic, or in Ca^{2+} signaling for only short periods on a thin basement membrane coating. Others have shown that HSG cells require several days of growth on a thicker basement membrane substratum to promote amylase production and cell polarization (Hoffman et al., 1996). Secretory vesicles (Royce et al., 1993) are detected together with the formation of acinar-like structures.

The discovery of STIM1 and, very recently, Orai1 as being, together, essential for SOC influx (Peinelt et al., 2006; Soboloff et al., 2006) opens new areas of investigation. STIM1 undergoes ER to PM or near-PM translocation regulated by its Ca^{2+}-binding EF hand (Liou et al., 2005; Zhang et al., 2005). Orai1 is thought to form or help form the Ca^{2+} channel. TRPC1 is considered to be a SOC candidate (Ambudkar, 2006). TRPC1 is endogenously expressed in HSG cells, and when stably overexpressed enhances SOC influx, unlike overexpression of TRPC3 (Liu et al., 2000). Why would depletion of TRPC1 have no effect on lacritin-induced Ca^{2+} influx, NFATC1 translocation, or mitogenesis; or on SOC in the thapsigargin-treated cells of Roos et al. (2005) and Liou et al. (2005)? Possibly another TRPC compensates (i.e., TRPC3 at low levels is store operated; Vazquez et al., 2003), although SOC was not affected by coordinated targeting of all three *Drosophila melanogaster* trp genes (Roos et al., 2005). We ruled out the possibility that siRNA depletion was not complete (Fig. S3 A). TRPC1 may turnover relatively slowly and, thus, protein levels might take longer to lower, yet recent 80 nM siRNA depletion of TRPC1 protein in IEC cells was almost and entirely complete by 24 and 48 h, respectively (Marasa et al., 2006). Because we have not examined the effect of siSTIM1 or siTRPCI on thapsigargin-stimulated Ca^{2+} entry or NFAT activation, it is possible that the mechanism observed is relatively specific for lacritin. FBS stimulation was unaffected by both depletions. Early studies suggested that STIM1 overexpression affects cell phenotype and adhesion without diminishing viability (Oritani and Kincade, 1996) or, contrastingly, is apoptotic (Manji et al., 2000). We observed no apparent affect of STIM1 depletion on adhesion, and have found lacritin to be antiapoptotic (unpublished data). Future studies seeking to move lacritin from HSG cells to mouse models and primary cultures of dispersed glands (Luo et al., 2001) provide an opportunity to explore these interrelated observations. How does lacritin selectively target some, but not other, epithelia? New data suggests a novel mechanism in which extracellular HPSE unblocks a lacritin-binding site on the core protein of SDC1 (Ma et al., 2006). This transforms a widely expressed cell surface proteoglycan into a selective coreceptor that hypothetically presents lacritin to a lower affinity signaling receptor. siRNA depletion of HPSE abrogates lacritin-dependent, but not EGF-dependent, mitogenesis. In pull-down assays, SDC1 core protein binding maps to lacritin's mitogenic domain. Neither syndecans-2 nor -4 bind lacritin, in keeping with poor ectodomain conservation. Immunostaining for SDC1 in human lacrimal gland reveals a basolateral distribution that appears to reach to the apical surface (unpublished data). HPSE cleavage of heparan sulfate is associated with follicular stem cell migration in mouse skin (Zcharia et al., 2005) and when added exogenously inhibits stroma-induced quiescence of bone marrow stem cells (Gordon et al., 1997). Whether lacritin can act on corneal/limbal stem cells as it flows onto the eye is not known. Lacritin's HPSE-dependent binding of SDC1 ectodomain contrasts with heparan sulfate–binding growth factors such as FGF's, Wnts, and hedgehogs, which do not appear to discriminate among syndecans or other heparan sulfate proteoglycans. By limiting availability of HPSE, lacritin can hypothetically target fewer differentiated epithelia as it flows downstream.

Like lacritin, several other mitogens are secreted apically, including TGFβ1 (Murphy et al., 2004), neurotrophin (Yeaman et al., 1997), and VEGF (Hornung et al., 1998), as well as EGFs, TGFs, HGF, and FGFs, and have all been detected in lacrimal and salivary ductal secretions. Although apical membranes are not commonly considered to be receptor-rich, CD-44 (mammary gland, salivary gland, and pancreas) nucleates MMP7 and pro–HB-EGF in an apical complex with ErbB4 are necessary for epithelial cell survival (for review see Wang and Laurie, 2004). The M3 muscarinic receptor is apically concentrated in exocrine pancreas (Luo et al., 2005), and polarized MDCK cells sort nerve growth factor receptor to the apical surface (Yeaman et al., 1997). Such outward mitogenic flow from secretory cells through ducts of nongermative epithelia could potentially regulate secretory physiology and cellular renewal.

Materials and methods

Cell lines

Human salivary ductal cells (HSG) were expanded in DME with 10% FCS (Sanghi et al., 2001) or, for mitogenesis experiments, in MEM (Eagle's α modification). Other cells were grown as per American Type Culture Collection guidelines. All media were purchased from Invitrogen.

Lacritin constructs and purification

A 363-bp region of DNA coding for intact mature lacritin without signal peptide was PCR-amplified from lacritin cDNA and subcloned into pTYB1 (New England Biolabs, Inc.) as the lacritin–intein fusion plasmid "pLAC." Respective additions of SapI to forward primer 5′-GGTGGTCATATGGAAGATGCC-3′ and of NdeI to reverse primer 5′-GGTGGTTGCTCTTCCGCATGCCCATGG-3′ facilitated subcloning. C-terminal deletions of 5, 10, 15, 20, 25, and 59 aa were generated using forward primer 5′ -GGTGGTTGCTCTTCCAACTATTATTACTATGAAGATGCCTCCTCT-3′ and the reverse primers 5′-GGTGGTGAATTCTCATAGACTGAATT-3′, 5′-GGTGGTGAATTCTCACAGTAATTTTTG-3′, 5′-GGTGGTGAATTCTCAAAATTCACTTCC-3′, 5′-GGTGGTGAATTCTCATTCGATGAATTC-3′, 5′-GGTGGTGAATTCTCATTCACCTGGCA-3′, and 5′-GGTGGTGAATTCTCACTGCCTGCTTG-3′, respectively. Amplicons were directionally subcloned into pTYB11 using SapI and EcoRI as "pLAC/C-5 – pLAC/C-59." Forward and reverse primers for the N-24–terminal deletion were 5′-GGTGGTTGCTCTTCCAACATCTCAGGTCCAGCAGAAC-3′ and 5′-GGTGGTTGCTCTTCCGCATGCCCATGG-3′, respectively, creating the plasmid "pLAC/N-24." All constructs were verified by sequencing.

Bacterial protein expression was performed using standard procedures. Cleared cell lysates were loaded on chitin columns (IMPACT-CN System; New England Biolabs, Inc.) and equilibrated with 50 mM Tris, 0.5 M NaCl, pH 8.0, followed by 20-column volumes of washing, elution with 50 mM DTT for 16 h at RT in the same buffer, extensive dialysis against PBS (4°C), and protein quantitation. The size of lacritin from pLAC is 18 kD (12.3 kD predicted) versus 23 kD from pET28b (18.4 kD predicted with His tag plus signal peptide; previously indicated in error as greater in Sanghi et al. [2001]). Mass spectrometry sequencing, and immunoblotting confirmed protein identity. Circular dichroism analysis was performed in a spectropolarimeter running numerical analysis software (AVIV 215 and Igor Pro, respectively; both Wyatt Technology, Corp.).

Phosphotyrosine blotting and mitogenesis

Cells in serum-containing media were seeded overnight in 24-well plates at a density of 0.5×10^5 cells/mm^2 corresponding to 20–30% confluency after cell attachment (see optimization experiments in Fig. S1). Cells were then incubated in serum-free (SF) media without supplements for 24 h (phosphotyrosine), or washed with SF media without supplements three times (mitogenesis) and then incubated with lacritin (1–1,000 nM). In positive controls, cells were incubated with 1.6 nM EGF or 10% FBS. In negative controls, cells were incubated with BSA or without additive in SF media without supplements. Duration of incubation with lacritin, or with negative or positive controls, was for the indicated times (phosphotyrosine) or for 30 h (mitogenesis). In phosphotyrosine assays, cells were extracted in 1% NP-40 containing sodium vanadate, 5 mg/ml DTT, protease inhibitors, 50 mM Hepes, 100 mM NaCl, and 2 mM EDTA; the cells were then separated by 2 mg/ml 10% SDS PAGE, transferred, and blotted. Antiphosphotyrosine antibody (P-Tyr-100), anti–phoshpo-PKCαβII, anti-PKCα, anti-p44/p42 MAPK, anti-PLCγ2, and anti-GSK were purchased from Cell Signaling Technology. After washing, bound antibodies were detected with peroxidase-labeled secondary antibody and ECL. For mitogenesis, 2 μCi/ml [^{3}H]TdR was added for an additional 6 h. Labeling was stopped with ice-cold PBS and followed by addition of cold and RT TCA (10%) for 10 min each. After washing, radioactivity was quantitated in a scintillation counter. For PKCα depletion, a pool of four PKCα-specific siRNAs or individual siRNAs (100 nM; Millipore) were transfected into HSG cells via Lipofectamine 2000 in Opti-MEMI Reduced Serum medium (Invitrogen) in the absence of serum and antibiotics, according to the manufacturer's instructions. PKCα depletion was confirmed by Western blotting. Other cells were transfected with pools of NFATC1-, TRPC1-, mTOR-, or STIM1-specific siRNAs. In negative controls, cells were transfected with a pool of four lamin-specific siRNAs (all 100 nM; Dharmacon Inc.). 72 h after transfection, mitogenesis was assessed by coaddition of 10 nM lacritin and 2 mCi/ml [^{3}H]TdR (GE Healthcare) for 24 h. For rapamycin and CsA inhibition, cells that had been incubated in SF media overnight were treated with 1 μM CsA (Sigma-Aldrich) for 5 h, 100 nM rapamycin (Calbiochem) for 15 min, or both; they were then stimulated with 10 nM lacritin in the same medium with 2 mCi/ml [^{3}H]TdR for an additional 24 h. For RT-PCR analyses, total RNAs from cells were reverse transcribed (RETROscript; Ambion) and subjected to PCR using Super Taq DNA polymerase (Ambion) for 10 min at 95°C, followed by 35 cycles for 45 s at 95°C, 45 s at 55°C, and 90 s at 72°C. Primers used were: (COX2 forward) 5′-AATTTAACACCCTCTATCACTGGC-3′ and 5′-AATTGAGGCAGTGTTGATGATTTGAA-3′ (COX2 reverse); (IL-6 forward) 5′-GACAGCCACTCACCTCTTCA-3′, and (IL-6 reverse) 5′-TCTGGCTTGTTCCTCACTACTCTCA-3′; and (GAPDH forward) 5′-GTCGGAGTCAACGGATTTGGT-3′ and (GAPDH reverse) 5′-TCATGAGCCCTTCCACGATGCC-3′. PLD activity was measured as previously described by Santy and Casanova (2001). For immunoprecipitation experiments, cells were lacritin treated for 15 min, lysed with protease inhibitors, spun, precleared using protein A–Sepharose, and then subjected to anti-PLCγ2 affinity precipitation. Precipitates were separated by 10% SDS-PAGE gels, transferred, and blotted using standard assays.

Ca^{2+} translocation and colocalization analyses

Cells were seeded at 1.4 or 0.7×10^4 cells/mm^2 on Matrigel-coated coverslips (100 μg/ml; BD Biosciences) to respectively achieve 70–80% confluency after overnight or 48-h growth in 6-well plates containing phenol red–free DME with 10% FCS. Cells were washed repeatedly in Ca^{2+}/phenol red–free HBSS with 20 mM Hepes (Invitrogen), and then incubated for 10 min in the same solution containing 1 μM U73122, 1 μM U73343 (BIOMOL Research Labs), 1 μM Go 6976, or 10 μM nifedipine (Calbiochem); or for control in vehicle (DMSO/Pluronic diluted to same level in inhibitor solution) alone. Other cells were incubated (0.7×10^4 HSG cells/mm^2 overnight plating) with 100 ng/ml PTX (Calbiochem) in phenol red–free DME with 10% FCS or with vehicle alone). Cells were washed with Ca^{2+}/phenol red–free HBSS and 20 mM Hepes, and then incubated for 1 h at RT with the same solution containing Fluo-4 AM at 4 μM (FluoroPure grade [Invitrogen] dissolved in DMSO plus 20% Pluronic F-127). Cells were washed three times for 60 min at RT with Ca^{2+}/phenol red–free HBSS with 5 mM Ca^{2+} or EGTA. Temperature was stabilized for 5 min at 37°C, and then coverslips were placed on the stage of an epifluorescent microscope (TE300; Nikon; located in the W.M. Keck Center for Cellular Imaging at the University of Virginia). TE300 was coupled to a Radiance 2100 confocal/multiphoton system using a Plan Fluor 60×, NA 1.4, oil IR objective lens (both from Bio-Rad Laboratories). Cells were subjected to a 488-nm argon laser light source with emission at 528 nm. Baseline monitoring was followed by addition of lacritin or the deletion fragments in phenol red–free HBSS. Images were acquired at 2–3-s intervals using LaserSharp2000 software (Bio-Rad Laboratories) and stored on disc for later analysis. Cells were depleted of STIM1 or TRPC1 by siRNA and stimulated with lacritin. In other assays, cells were treated with 10 μM BHQ for 15 min in Ca^{2+}/phenol red–free HBSS and stimulated with 10 nM lacritin. Later, 1.5 mM Ca^{2+} was added. For translocation assays, HSG cells on Matrigel-coated coverslips with or without inhibitors were treated with 10 nM lacritin or positive control, 200 nM PMA, or vehicle for 15 min, washed with PBS, formaldehyde-fixed, blocked with PBS containing 1% BSA and 10% goat serum, and incubated with anti-PKCα (C-20) or anti-NFATC1 (mAb 7A6; both from Santa Cruz Biotechnology, Inc.), followed by secondary Cy3-, FITC-, or Alexa Fluor 488–labeled antibodies and confocal microscopic visualization (Radiance 2100; Bio-Rad Laboratories). In colocalization studies, we used anti-PKCα (H-7; Santa Cruz Biotechnology, Inc.), anti-PLCγ2 (Cell Signaling Technology), and purified anti-PLD1 (from serum 41) provided by D. Shields (Albert Einstein College of Medicine of Yeshiva University, New York, NY). For NFATC1 blots, nuclei from lacritin-treated cells without or with inhibitors were purified, separated by SDS-PAGE, blotted, and detected with anti-NFATC1. As loading control, anti-Ran antibody was provided by I. Macara (University of Virginia, Charlottesville, VA). For measurement of IP_3 generation, HSG cells were incubated SF in 2-[^{3}H]myo-inositol for 24 h, washed, and treated with 10 nM lacritin or C-25 or 100 μM carbachol. Processing was as previously described by Webb et al. (1995). Measurement of calcineurin activity used the Calcineurin Cellular Activity Assay kit (Calbiochem). 80–90%-confluent HSG cells in 6-well plates were treated in triplicate and collected for assay of calcineurin activity.

Statistical analyses

All experiments were performed at least three times. Data are presented as the mean ± the SEM.

Online supplemental material

Fig. S1 (A and B) display lacritin mitogenic time course and confluency analyses, respectively. Fig. S2 documents lacritin-dependent generation

of IP_3. Fig. S3 analyzes lacritin-dependent Ca^{2+} influx in cells depleted of STIM1 or TRPC1. Fig. S4 quantitates the proportion of lacritin-treated cells in which NFAT is nuclear. Cells were treated with 10 nM lacritin for 15 min. Nuclear localization was confirmed by DAPI. Normal, U73122-inhibited, and STIM1- and TRPC1-depleted cells are compared. Online supplemental material is available at http://www.jcb.org/cgi/content/full/jcb.200605140/DC1.

We thank Jim Casanova, Barry Gumbiner, Sally Parsons, and Martin Schwartz for critically reading the manuscript. Jiahu Wang performed lacritin Ca^{2+} signaling, visualized translocations, and helped write the article. Ningning Wang generated siRNA-depleted cells, studied PLD, mitogenic, and calcineurin activities, performed coimmunoprecipitations and all blotting, and helped write the article. Jinling Xi did carbachol Ca^{2+} and lacritin dose–response signaling. Staci Walton discovered the biphasic mitogenic response and did ptyr studies. Isa Hussaini helped with ptyr and signaling. Robert McKown, Ronald Raab, and George Coffman designed and generated lacritin constructs. Peisong Ma did IP_3 assays. Shannon Beck performed CD and helical wheel analysis. Gordon Laurie conceived the experiments and wrote the article.

S.L. Beck was supported by National Institutes of Health (NIH) grant T32 GM08715. This work was supported by NIH grant RO1 EY13143 (to G.W. Laurie).

We have no competing financial interests.

Submitted: 23 May 2006
Accepted: 18 July 2006

References

Ambudkar, I.S. 2006. Ca(2+) signaling microdomains: platforms for the assembly and regulation of TRPC channels. *Trends Pharmacol. Sci.* 27:25–32.

Barden, J.A., R.M. Cuthbertson, W. Jia-Zhen, J.M. Moseley, and B.E. Kemp. 1997. Solution structure of parathyroid hormone related protein (residues 1-34) containing an Ala substituted for an Ile in position 15 (PTHrP[Ala15]-(1-34)). *J. Biol. Chem.* 272:29572–29578.

Barker, S.A., K.K. Caldwell, J.R. Pfeiffer, and B.S. Wilson. 1998. Wortmannin-sensitive phosphorylation, translocation, and activation of PLCgamma1, but not PLCgamma2, in antigen-stimulated RBL-2H3 mast cells. *Mol. Biol. Cell*. 9:483–496.

Butzal, M., S. Loges, M. Schweizer, U. Fischer, U.M. Gehling, D.K. Hossfeld, and W. Fiedler. 2004. Rapamycin inhibits proliferation and differentiation of human endothelial progenitor cells in vitro. *Exp. Cell Res.* 300:65–71.

Caetano, M.S., A. Vieira-de-Abreu, L.K. Teixeira, M.B. Werneck, M.A. Barcinski, and J.P. Viola. 2002. NFATC2 transcription factor regulates cell cycle progression during lymphocyte activation: evidence of its involvement in the control of cyclin gene expression. *FASEB J.* 16:1940–1942.

Chang, C.P., J.R. Neilson, J.H. Bayle, J.E. Gestwicki, A. Kuo, K. Stankunas, I.A. Graef, and G.R. Crabtree. 2004. A field of myocardial-endocardial NFAT signaling underlies heart valve morphogenesis. *Cell*. 118:649–663.

Davies, S.P., H. Reddy, M. Caivano, and P. Cohen. 2000. Specificity and mechanism of action of some commonly used protein kinase inhibitors. *Biochem. J.* 351:95–105.

Dor, Y., J. Brown, O.L. Martinez, and D.A. Melton. 2004. Adult pancreatic beta-cells are formed by self-duplication rather than stem-cell differentiation. *Nature*. 429:41–46.

Fang, Y., I.H. Park, A.L. Wu, G. Du, P. Huang, M.A. Frohman, S.J. Walker, H.A. Brown, and J. Chen. 2003. PLD1 regulates mTOR signaling and mediates Cdc42 activation of S6K1. *Curr. Biol.* 13:2037–2044.

Foster, D.A., and L. Xu. 2003. Phospholipase D in cell proliferation and cancer. *Mol. Cancer Res.* 1:789–800.

Gangloff, Y.G., M. Mueller, S.G. Dann, P. Svoboda, M. Sticker, J.F. Spetz, S.H. Um, E.J. Brown, S. Cereghini, G. Thomas, and S.C. Kozma. 2004. Disruption of the mouse mTOR gene leads to early postimplantation lethality and prohibits embryonic stem cell development. *Mol. Cell. Biol.* 24:9508–9516.

Gordon, M.Y., J.L. Lewis, S.B. Marley, F.H. Grand, and J.M. Goldman. 1997. Stromal cells negatively regulate primitive haemopoietic progenitor cell activation via a phosphatidylinositol-anchored cell adhesion/signalling mechanism. *Br. J. Haematol.* 96:647–653.

Hoffman, M.P., M.C. Kibbey, J.J. Letterio, and H.K. Kleinman. 1996. Role of laminin-1 and TGF-beta 3 in acinar differentiation of a human submandibular gland cell line (HSG). *J. Cell Sci.* 109:2013–2021.

Holz, M.K., and J. Blenis. 2005. Identification of S6 kinase 1 as a novel mammalian target of rapamycin (mTOR)-phosphorylating kinase. *J. Biol. Chem.* 280:26089–26093.

Hornung, D., D.I. Lebovic, J.L. Shifren, J.L. Vigne, and R.N. Taylor. 1998. Vectorial secretion of vascular endothelial growth factor by polarized human endometrial epithelial cells. *Fertil. Steril.* 69:909–915.

Hu, T., and J.H. Exton. 2004. Protein kinase Calpha translocates to the perinuclear region to activate phospholipase D1. *J. Biol. Chem.* 279:35702–35708.

Jung, D.W., D. Hecht, S.W. Ho, B.C. O'Connell, H.K. Kleinman, and M.P. Hoffman. 2000. PKC and ERK1/2 regulate amylase promoter activity during differentiation of a salivary gland cell line. *J. Cell. Physiol.* 185:215–225.

Lane, H.A., A. Fernandez, N.J. Lamb, and G. Thomas. 1993. p70s6k function is essential for G1 progression. *Nature*. 363:170–172.

Lee, S.J., K. Lee, X. Yang, C. Jung, T. Gardner, H.S. Kim, M.H. Jeng, and C. Kao. 2003. NFATc1 with AP-3 site binding specificity mediates gene expression of prostate-specific-membrane-antigen. *J. Mol. Biol.* 330:749–760.

Liou, J., M.L. Kim, W.D. Heo, J.T. Jones, J.W. Myers, J.E. Ferrell Jr., and T. Meyer. 2005. STIM is a Ca2+ sensor essential for Ca2+-store-depletion-triggered Ca2+ influx. *Curr. Biol.* 15:1235–1241.

Liu, C.H., S.-H. Chang, K. Narko, O.C. Trifan, M.-T. Wu, E. Smith, C. Haudenschild, T.F. Lane, and T. Hla. 2001. Overexpression of cyclooxygenase-2 is sufficient to induce tumorigenesis in transgenic mice. *J. Biol. Chem.* 276:18563–18569.

Liu, X., W. Wang, B.B. Singh, T. Lockwich, J. Jadlowiec, B. O'Connell, R. Wellner, M.X. Zhu, and I.S. Ambudkar. 2000. Trp1, a candidate protein for the store-operated Ca(2+) influx mechanism in salivary gland cells. *J. Biol. Chem.* 275:3403–3411.

Luo, X., J.Y. Choi, S.B. Ko, A. Pushkin, I. Kurtz, W. Ahn, M.G. Lee, and S. Muallem. 2001. HCO3-salvage mechanisms in the submandibular gland acinar and duct cells. *J. Biol. Chem.* 276:9808–9816.

Luo, X., D.M. Shin, X. Wang, S.F. Konieczny, and S. Muallem. 2005. Aberrant localization of intracellular organelles, Ca2+ signaling, and exocytosis in Mist1 null mice. *J. Biol. Chem.* 280:12668–12675.

Ma, P., S.L. Beck, R.W. Raab, R.L. McKown, G.L. Coffman, A. Utani, W.J. Chirico, A.C. Rapraeger, and G.W. Laurie. 2006. Heparanase deglycanation of syndecan-1 is required for binding of epithelial-restricted prosecretory mitogen "lacritin". *J. Cell Biol*. In press.

Marasa, B.S., J.N. Rao, T. Zou, L. Liu, K.M. Keledjian, A.H. Zhang, L. Xiao, J. Chen, D.J. Turner, and J.-Y. Wang. 2006. Induced TRPC1 expression sensitizes intestinal epithelial cells to apoptosis by inhibiting NF-kappaB activation through Ca2+ influx. *Biochem. J.* 397:77–87.

Manji S.S., N.J. Parker, R.T. Williams, L. van Stekelenburg, R.B. Pearson, M. Dziadek, P.J. Smith. 2000. STIM1: a novel phosphoprotein located at the cell surface. *Biochim. Biophys. Acta.* 1481:147–155.

Messier, B., and C.P. Leblond. 1960. Cell proliferation and migration as revealed by radioautography after injection of thymidine-H3 into male rats and mice. *Am. J. Anat.* 106:247–285.

Murphy, S.J., J.J. Dore, M. Edens, R.J. Coffey, J.A. Barnard, H. Mitchell, M. Wilkes, and E.B. Leof. 2004. Differential trafficking of transforming growth factor-beta receptors and ligand in polarized epithelial cells. *Mol. Biol. Cell*. 15:2853–2862.

Murre, C., P.S. McCaw, H. Vaessin, M. Caudy, L.Y. Jan, Y.N. Jan, C.V. Cabrera, J.N. Buskin, S.D. Hauschka, A.B. Lassar, et al. 1989. Interactions between heterologous helix-loop-helix proteins generate complexes that bind specifically to a common DNA sequence. *Cell*. 58:537–544.

Neufang, G., G. Furstenberger, M. Heidt, F. Marks, and K. Muller-Decke. 2001. Abnormal differentiation of epidermis in transgenic mice constitutively expressing cyclooxygenase-2 in skin. *Proc. Natl. Acad. Sci. USA*. 98:7629–7634.

Oritani, K., and P.W. Kincade. 1996. Identification of stromal cell products that interact with pre-B cells. *J. Cell Biol.* 134:771–782.

Peinelt, C., M. Vig, D.L. Koomoa, A. Beck, M.J. Nadler, M. Koblan-Huberson, A. Lis, A. Fleig, R. Penner, and J.P. Kinet. 2006. Amplification of CRAC current by STIM1 and CRACM1 (Orai1). *Nat. Cell Biol.* 8:771–773.

Porter, D., S. Weremowicz, K. Chin, P. Seth, A. Keshaviah, J. Lahti-Domenici, Y.K. Bae, C.L. Monitto, A. Merlos-Suarez, J. Chan, et al. 2003. A neural survival factor is a candidate oncogene in breast cancer. *Proc. Natl. Acad. Sci. USA*. 100:10931–10936.

Putney, J.W., Jr. 2005. Capacitative calcium entry: sensing the calcium stores. *J. Cell Biol.* 169:381–382.

Rizvi, A.Z., and M.H. Wong. 2005. Epithelial stem cells and their niche: there's no place like home. *Stem Cells*. 23:150–165.

Rommel, C., S.C. Bodine, B.A. Clarke, R. Rossman, L. Nunez, T.N. Stitt, G.D. Yancopoulos, and D.J. Glass. 2001. Mediation of IGF-1-induced skeletal myotube hypertrophy by PI(3)K/Akt/mTOR and PI(3)K/Akt/GSK3 pathways. *Nat. Cell Biol.* 3:1009–1013.

Roos, J., P.J. DiGregorio, A.V. Yeromin, K. Ohlsen, M. Lioudyno, S. Zhang, O. Safrina, J.A. Kozak, S.L. Wagner, M.D. Cahalan, et al. 2005. STIM1,

an essential and conserved component of store-operated Ca^{2+} channel function. *J. Cell Biol.* 169:435–445.

Royce, L.S., M.C. Kibbey, P. Mertz, H.K. Kleinman, and B.J. Baum. 1993. Human neoplastic submandibular intercalated duct cells express an acinar phenotype when cultured on a basement membrane matrix. *Differentiation*. 52:247–255.

Sacco, A., R. Doyonnas, M.A. LaBarge, M.M. Hammer, P. Kraft, and H.M. Blau. 2005. IGF-I increases bone marrow contribution to adult skeletal muscle and enhances the fusion of myelomonocytic precursors. *J. Cell Biol.* 171:483–492.

Sanghi, S., R. Kumar, A. Lumsden, D. Dickinson, V. Klepeis, V. Trinkaus-Randall, H.F. Frierson Jr., and G.W. Laurie. 2001. cDNA and genomic cloning of lacritin, a novel secretion enhancing factor from the human lacrimal gland. *J. Mol. Biol.* 310:127–139.

Santy, L.C., and J.E. Casanova. 2001. Activation of ARF6 by ARNO stimulates epithelial cell migration through downstream activation of both Rac1 and phospholipase D. *J. Cell Biol.* 154:599–610.

Sinor, A.D., and L. Lillien. 2004. Akt-1 expression level regulates CNS precursors. *J. Neurosci.* 24:8531–8541.

Sheldahl, L.C., M. Park, C.C. Malbon, and R.T. Moon. 1999. Protein kinase C is differentially stimulated by Wnt and Frizzled homologs in a G-protein-dependent manner. *Curr. Biol.* 9:695–698.

Siemeister, G., D. Marme, and G. Martiny-Baron. 1998. The alpha-helical domain near the amino terminus is essential for dimerization of vascular endothelial growth factor. *J. Biol. Chem.* 273:11115–11120.

Slice, L.W., T. Chiu, and E. Rozengurt. 2005. Angiotensin II and epidermal growth factor induce cyclooxygenase-2 expression in intestinal epithelial cells through small GTPases using distinct signaling pathways. *J. Biol. Chem.* 280:1582–1593.

Smoot, M.E., E.J. Bass, S.A. Guerlain, and W.R. Pearson. 2005. A system for visualizing and analyzing near-optimal protein sequence alignments. *Inf. Visualiz.* 4:224–237.

Soboloff, J., M.A. Spassova, X.D. Tang, T. Hewavitharana, W. Xu, and D.L. Gill. 2006. Orai1 and STIM reconstitute store-operated calcium channel function. *J. Biol. Chem.* 281:20661–20665.

Tumbar, T., G. Guasch, V. Greco, C. Blanpain, W.E. Lowry, M. Rendl, and E. Fuchs. 2004. Defining the epithelial stem cell niche in skin. *Science*. 303:359–363.

Vazquez, G., B.J. Wedel, M. Trebak, G. St. John Bird, and J.W. Putney Jr. 2003. Expression level of the canonical transient receptor potential 3 (TRPC3) channel determines its mechanism of activation. *J. Biol. Chem.* 278:21649–21654.

Wang, J., and G.W. Laurie. 2004. Organogenesis of the exocrine gland. *Dev. Biol.* 273:1–22.

Webb, D.J., I.M. Hussaini, A.M. Weaver, T.L. Atkins, C.T. Chu, S.V. Pizzo, G.K. Owens, and S.L. Gonias. 1995. Activated alpha 2-macroglobulin promotes mitogenesis in rat vascular smooth muscle cells by a mechanism that is independent of growth-factor-carrier activity. *Eur. J. Biochem.* 234:714–722.

Weigelt, B., A.J. Bosma, and L.J.J. Van't Veer. 2003. Expression of a novel lacrimal gland gene lacritin in human breast tissues. *J. Cancer Res. Clin. Oncol*. 129:735–736.

Wing, L.Y., H.M. Chen, P.C. Chuang, M.H. Wu, and S.J. Tsai. 2005. The mammalian target of rapamycin-p70 ribosomal S6 kinase but not phosphatidylinositol 3-kinase-Akt signaling is responsible for fibroblast growth factor-9-induced cell proliferation. *J. Biol. Chem.* 280:19937–19947.

Yang, T.T., Q. Xiong, I.A. Graef, G.R. Crabtree, and C.W. Chow. 2005. Recruitment of the extracellular signal-regulated kinase/ribosomal S6 kinase signaling pathway to the NFATc4 transcription activation complex. *Mol. Cell. Biol.* 25:907–920.

Yeaman, C., A.H. Le Gall, A.N. Baldwin, L. Monlauzeur, A. Le Bivic, and E. Rodriguez-Boulan. 1997. The *O*-glycosylated stalk domain is required for apical sorting of neurotrophin receptors in polarized MDCK cells. *J. Cell Biol.* 139:929–940.

Zcharia, E., D. Philp, E. Edovitsky, H. Aingorn, S. Metzger, H.K. Kleinman, I. Vlodavsky, and M. Elkin. 2005. Heparanase regulates murine hair growth. *Am. J. Pathol.* 166:999–1008.

Zhang, S.L., Y. Yu, J. Roos, J.A. Kozak, T.J. Deerinck, M.H. Ellisman, K.A. Stauderman, and M.D. Cahalan. 2005. STIM1 is a Ca2+ sensor that activates CRAC channels and migrates from the Ca2+ store to the plasma membrane. *Nature*. 437:902–905.